JACS
JOURNAL OF THE AMERICAN CHEMICAL SOCIETY
Article
pubs.acs.org/JACS

QM/MM Simulation (B3LYP) of the RNase A Cleavage-Transesterification Reaction Supports a Triester A_N + D_N Associative Mechanism with an O2′ H Internal Proton Transfer

Brigitta Elsässer,[†] Gregor Fels,[†] and John H. Weare*[,‡]

[†]Department of Chemistry, University of Paderborn, Warburgerstr. 100, D-33098 Paderborn, Germany

[‡]Department of Chemistry and Biochemistry, University of California San Diego, 9500 Gilman Dr. 92093 La Jolla, California, United States

Supporting Information

ABSTRACT: The mechanism of the backbone cleavage-transesterification step of the RNase A enzyme remains controversial even after 60 years of study. We report quantum mechanics/molecule mechanics (QM/MM) free energy calculations for two optimized reaction paths based on an analysis of all structural data and identified by a search for reaction coordinates using a reliable quantum chemistry method (B3LYP), equilibrated structural optimizations, and free energy estimations. Both paths are initiated by nucleophilic attack of the ribose O2′ oxygen on the neighboring diester phosphate bond, and both reach the same product state (PS) (a O3′−O2′ cyclic phosphate and a O5′ hydroxyl terminated fragment). Path 1, resembles the widely accepted dianionic transition-state (TS) general acid (His119)/base (His12) classical mechanism. However, this path has a barrier (25 kcal/mol) higher than that of the rate-limiting hydrolysis step and a very loose TS. In Path 2, the proton initially coordinating the O2′ migrates to the nonbridging O1P in the initial reaction path rather than directly to the general base resulting in a triester (substrate as base) A_N + D_N mechanism with a monoanionic weakly stable intermediate. The structures in the transition region are associative with low barriers (TS1 10, TS2 7.5 kcal/mol). The Path 2 mechanism is consistent with the many results from enzyme and buffer catalyzed and uncatalyzed analog reactions and leads to a PS consistent with the reactive state for the following hydrolysis step. The differences between the consistently estimated barriers in Path 1 and 2 lead to a 10^{11} difference in rate strongly supporting the less accepted triester mechanism.

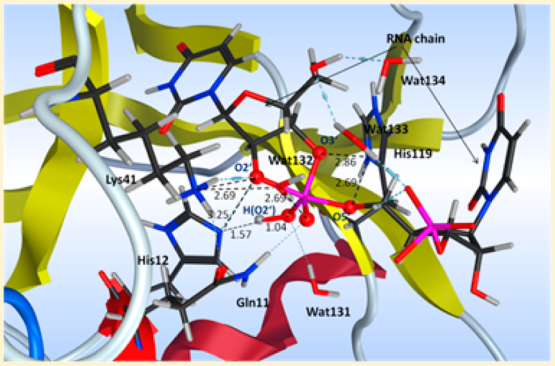

INTRODUCTION

Bovine pancreatic ribonuclease A (RNase A) accelerates the cleavage of single stranded RNA (behind each cytosyl and uridyl nucleotide) with rates in excess of 10^{12} times faster than the spontaneous uncatalyzed reaction.[1−4] As one of the earliest protein structures to be determined nearly 60 years ago, the RNase A reaction is arguably the most studied enzyme mechanism.[5−20] In addition to the direct observation of the enzyme reaction, a number of experimental studies of analogous reactions in homogeneous solutions that seek a deeper chemical understanding of this reactions remarkable acceleration have been reported in the organic and inorganic literature[2,7−10,21,22] (also starting nearly 60 years ago). There have also been a large number of theoretical studies (reviewed by Kamerlin et al.)[23] of similar solution reactions leading to an atomic level insight into the events controlling the reaction. Surprisingly, considering the great effort to understand this reaction and the broad importance of its mechanism, there are still major unsolved issues as to how the enzyme achieves this efficiency, and a mechanism that reconciles the results of both heterogeneous and homogeneous catalysis[1,9,10,15,21−25] has not been identified. The calculations reported here strongly support an alternative to the presently preferred classical mechanism.[1,27]

The overall RNase A reaction involves two separate steps (see Scheme S1).[1] In the first, the cleavage-transesterification step (the focus of this report), the 2′-hydroxyl oxygen adjacent to the 3′,5′ phosphodiester bond attacks the backbone phosphate yielding a cyclic 2′,3′-phosphate and a 5′ hydroxyl terminated fragment. In the second step, the ring is hydrolyzed (O2′−P bond broken) by water attack producing an O3′ phosphate product (see earlier communication).[26] While the general acid/base nature of the cleavage transesterification reaction (e.g., His12 the general base, His119 general acid) is universally accepted, the nature (structure, charge, and protonation) of the structures in the transition region of the reaction path presently cannot be directly observed[23] and are not well established even for this very well studied enzyme.[22,23,25] We show here that the nature of these structures (particularly the protonation of structure in the transition

Received: July 2, 2013
Published: December 30, 2013

   dx.doi.org/10.1021/ja406122c | J. Am. Chem. Soc. 2014, 136, 927−936

region) can affect the rate of the reaction by many orders of magnitude.

Two classes of mechanisms for the RNase A reactions have been extensively debated in the literature (particularly for analog reactions, see below).[1,6,9,22,23,25] The essential differences in these mechanisms involve the timing and destination of proton transfers along the reaction coordinate. In the TS of the classical mechanism[1] the nonbridging oxygens are unprotonated, unstable, and dianionic. While this reaction path is widely accepted for RNase A in the enzyme catalysis community,[24,27−29] the experimental support for this mechanism is not conclusive.[9,10,30]

An alternative path incorporating a triester mechanism has also been proposed.[9] In this mechanism in the transition region one of the nonbridging oxygens is protonated ("substrate as base mechanism")[23,31,32] leading to a monoanionic structure and a weakly stable intermediate. The calculations here strongly support the triester mechanism. Such a mechanism has been proposed and defended for the similar RNase T1 enzyme[33,34] providing additional support for this reaction path.

Mechanisms of analogous nonenzymatic phosphoryl transfer reactions (including transesterification) have been studied in the organic and inorganic literature for many years beginning with the seminal work of Westheimer[20] and including extensive experimental[1,6,8,10,12,19,25,30,35−41] and theoretical[4,5,18,23,42−55] studies by various research groups. These studies of uncatalyzed and buffer catalyzed transesterification and hydrolysis reactions have shown that such reactions have a complex reaction coordinate which may lead to orders of magnitude changes in reaction rate with changes in reaction conditions (e.g., pH, esterification level, leaving group, etc.). Consistent themes for the interpretation of these reactions were provided in the work of Westheimer and co-workers nearly 50 years ago.[16,20,56,57] These have been succinctly summarized in a recent article by Emilsson et al.[2] Mechanism suggested to be responsible for acceleration include: (in their notation)[2] γ-catalysis, deprotonation of the O2′ oxygen; δ-catalysis, neutralization of the O5′ oxygen on the leaving group; β-catalysis, neutralization of the charge (via protonation) on the nonbridging phosphate oxygens facilitating the possible formation of an intermediate state in a $A_N + D_N$ type[58] reaction (triester mechanism); and α-catalysis, development of molecular scaffolding to align the reactants for nucleophilic attack along a linear reaction coordinate. Similar themes in the context of theoretical simulations of solution reactions have been identified and recently reviewed by Kamerlin et al.[23]

Emilsson et al.[2] use observations from uncatalyzed reactions to estimate the maximum increase of rate possible from implementing each of these mechanisms. They propose that the optimal utilization of all of these mechanisms would provide an acceleration of 10^{19}. While there is general acceptance of the roles of these TS structures in the uncatalyzed reactions of small RNA oligomers,[10] there is controversy over how or even if the RNase A enzyme implements them. The direct observation of these mechanisms is still not possible because of the lack of probes of proton position and motion in the catalytic region.

Theoretical methods can supply additional highly detailed information about the events in chemical mechanisms.[23] In this article computational results are used to analyze the minimum energy reaction path for the transesterification step of the RNase A reaction. These calculations are based on a first principle quantum mechanics/molecule mechanics (QM/MM) theory[23,26,59−61] (electronic structure calculations at the B3LYP level see SI Section 2a) that we have successfully tested against structural measurements of similar systems[26,60] (see also SI). Our reaction path simulations implement a comprehensive representation of the fully solvated enzyme−substrate complex, full structural optimization, and free energy estimation along the reaction path. The structure of the enzyme substrate complex in the reactive state is developed from extensive docking studies (see below and the SI) of all available structural data and appears to agree well with this data (see SI Section 3b).

Through a fairly unbiased search (see SI Section 2) we have identified two minimum energy reaction paths in the catalyst, plus substrate, plus solution model. The first path, Path 1, is similar to the classical reaction mechanism. This is an A_ND_N mechanism with a loose TS (very weak O2′−P and O5′−P bonds in the TS) that utilizes His119 and His12 as the general acid and general base.[23,30] There are features of this path that agree with experimental observations. However, the activation barrier as estimated here is much higher than that reported for the hydrolysis step in RNase A.[1] Since the hydrolysis step is believed to be rate limiting for the RNase A reaction, this is not acceptable. In addition the dissociative TS character of this mechanism is quite different from those believed to be operative in the uncatalyzed reactions.[7,8,10]

The second mechanism, Path 2, follows an $A_N + D_N$ triester path with an associative weakly bound intermediate (INT). In this mechanism a proton originating via migration from the O2′ hydroxide coordinates one of the nonbridging phosphate oxygens to form a phosphate triester (β-catalysis).[2] The activation barriers along this path are low and consistent with the fast reaction rates of the enzyme. Remarkably considering the unguided nature of the calculation both Paths 1 and 2 lead to the same product state (PS), which is closely related to the reactant state (RS) we previously found for the hydrolysis step.[26] Path 2 implements all four of the strategies that have been identified in the uncatalyzed reactions, computational studies of simplified models, and analysis of the structures of TS analogs[3,8−10,28,30,45,47,63−66] and the proton transfers (PT) identified in the QM/MM studies of analogous solution reactions recently reviewed.[23] The differences between the calculated activation barriers in these two mechanisms would lead to a 10^{11} times faster reaction for the triester mechanism.

The fully optimized reaction paths we obtain provide details, e.g., timing of PT, movements of conserved residues, structures of the TS and estimates of intermediate stability (Path 2), and activation barrier heights, that are not available from observations or prior calculations of the RNase A mechanism and are important to the interpretation of the reaction. Both paths reported are thermally equilibrated minimum energy reaction paths allowing full atomic movement. Because the free energies of both paths were calculated with the same theory they may be reliably compared. Accepting that the present structural data is sufficient to analyze the reaction, the wider utilization of the catalytic machinery identified in the studies of uncatalyzed analogous reactions and the lower barriers of Path 2 suggests that it is the reaction mechanism responsible for the 10^{12} acceleration of the RNase A reaction.

Interest in the mechanism of the RNase A reaction has increased recently due to the growing interest in gene-specific therapy (development of ribosome mimics) that would require sequence-specific manipulation of RNA and because of the sequence selective catalytic nature of RNA components in

dx.doi.org/10.1021/ja406122c | J. Am. Chem. Soc. 2014, 136, 927−936

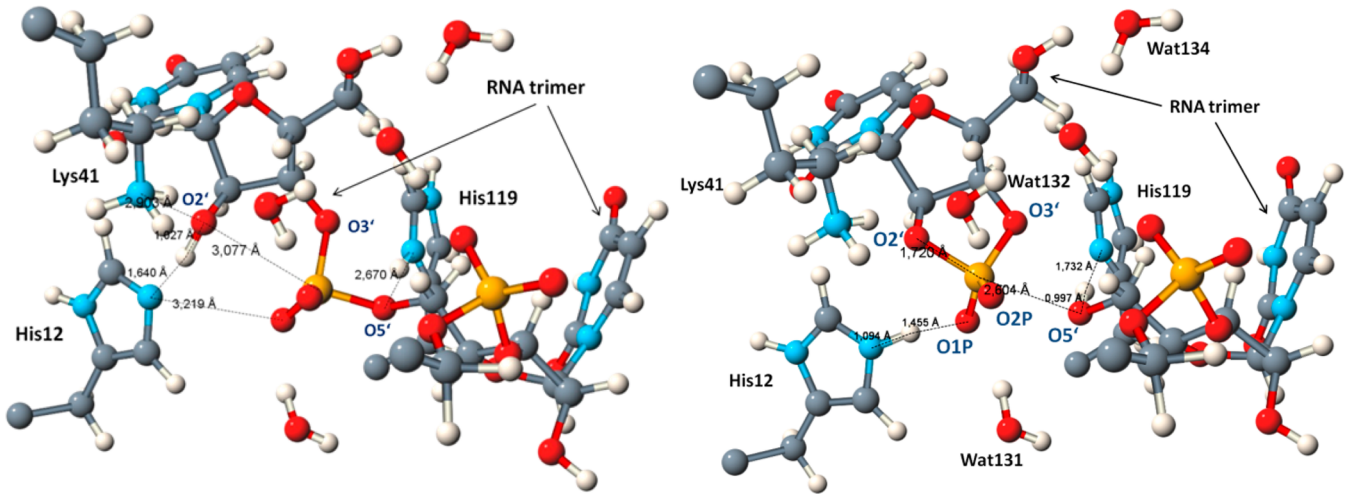

Figure 1. The structure of the reactant (left) and product (right) states with the most important H-bonding interactions illustrated.

Scheme 1. Path 1: Direct O2′ Proton Transfer

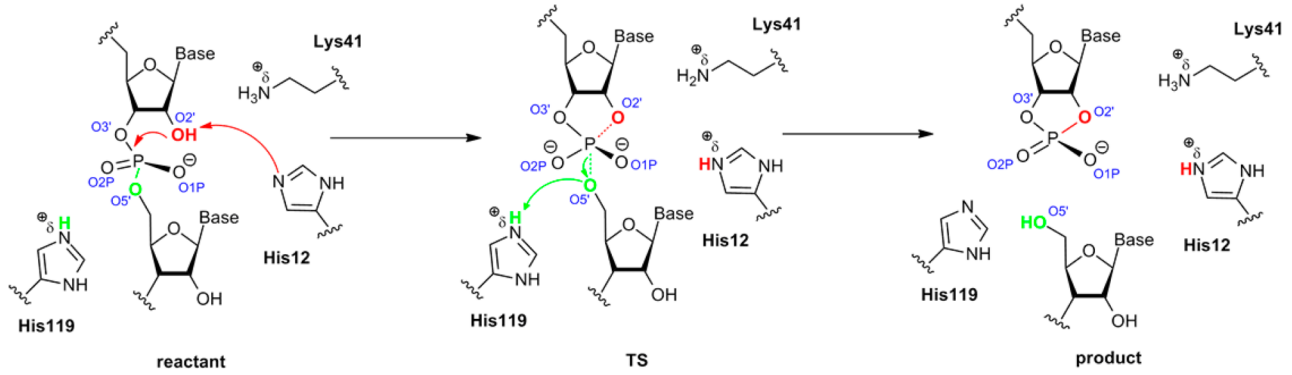

ribozymes which catalyze RNA backbone cleavage.[22,67] Four of the eight known ribozymes appear to cleave RNA via nucleophilic O2′ attack similar to that of the RNase A mechanism.[2,68] Additional attention has been generated by the recognition of the possibility of the important role of RNA in the evolution of self-replicating biological systems.[69−72]

RESULTS AND DISCUSSION

The theoretical tools that have been used in these calculations are discussed in detail in the methods section in the SI (Section 2) and in prior publications.[73−78] In this study these are applied to the cleavage-transesterification reaction in the enzyme system containing the enzyme/RNA complex fully solvated in a discrete water representation of the solution. The analysis implements a comprehensive effort to use all available structural data to define the reactive enzyme substrate complex; a QM/MM type calculation[23,46] implementing an accurate first-principle-based electronic structure calculation (B3LYP) to estimate the interactions in the catalytic cell represented by a large QM region ((117 atoms) required to reliably describe the enzyme/substrate complex), see SI, Section 2; a minimally biased search method to identify reaction mechanisms; thermal equilibration and nudged elastic bend (NEB)[79] structural optimization with full flexibility of the protein and substrate, including all Coulomb interactions between the QM and MM regions;[23] and free energy calculations along the reaction path.

As discussed by Klähn et al.[80] the minimum energy pathways in the QM region may be significantly affected by the structure of the surrounding protein and solution. In this work we iteratively thermally averaged the structure in the MM region with reoptimization of the QM structure at each position in the reaction path. This is described in the SI (Section 2) and previous references.[60,76,78] In prior work similar methods have been used to calculate the structure of TS analogs (PDB code: 1RUV)[64] for the hydrolysis step with excellent agreement[26] including direct comparisons of calculations with X-ray structure of the analog substrate.[64]

Development of the Reactant State (RS) Structure of the RNase A/RNA Complex. To develop a reaction mechanism for the transesterification reaction it is necessary to have a reliable initial RS (structure of the active enzyme substrate complex before reaction). For many problems reactive state information is available from some observed analog structure along the reaction pathway (e.g., a high resolution X-ray structure of an inhibited reaction[81] or a TS analog).[64]

For the RNase A enzyme this type of information is available only for the hydrolysis step.[26,82] To provide a starting structure for the transesterification reaction we used information from these structures as much as possible and in addition carried out an extensive structural search using a combination of docking algorithms and QM/MM optimizations with validation from the structures of analogous systems[81] (RNase A−DNA single strand (CA) complex (Section 3, SI)).[83]

This strategy was then applied to produce a preliminary candidate for the RS structure of the enzyme plus the RNA

dx.doi.org/10.1021/ja406122c | J. Am. Chem. Soc. 2014, 136, 927−936

Scheme 2. Path 2: Calculated Lower Energy Path for the Triester-Like Mechanism

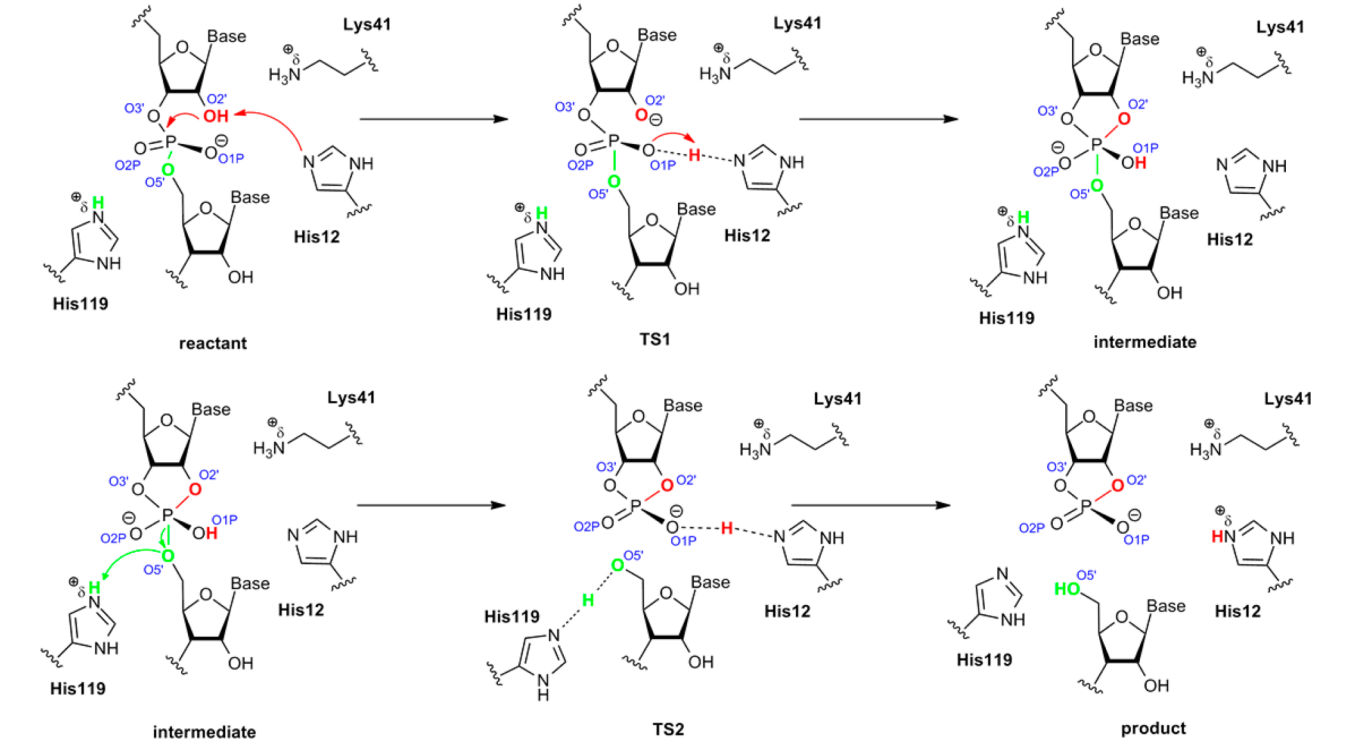

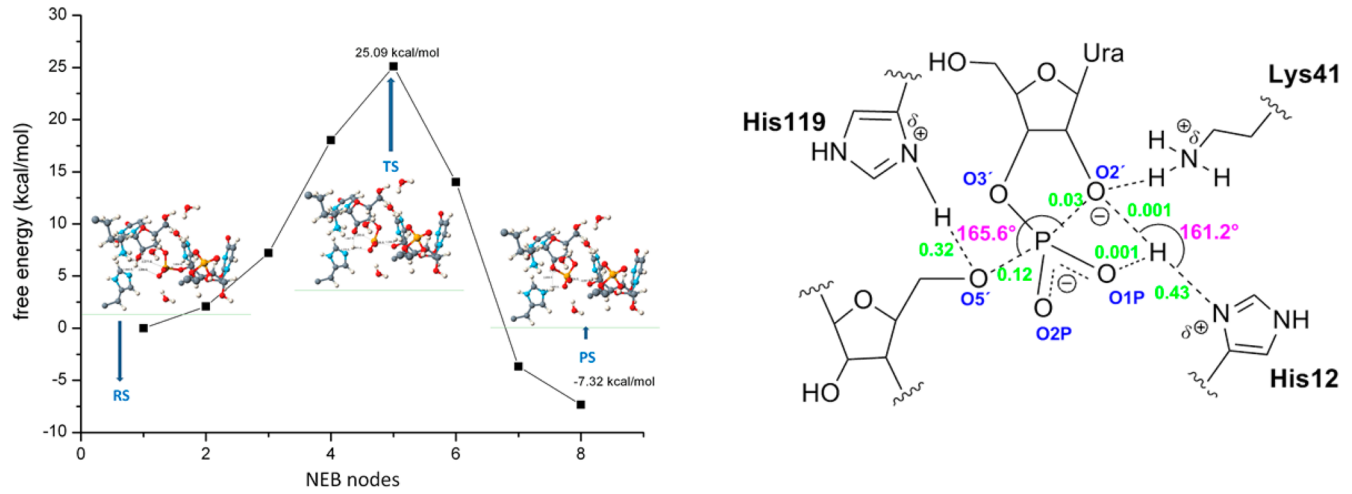

Figure 2. (left) Free energy profile of Path 1. (left) TS structure (right). The BO[62] are shown in green, and the relevant bond angles are purple (points are NEB nodes (see SI, Section 2d).

(UUU) substrate complex. Extensive iterative thermal averaging of this structure was carried out to ensure that the MM structure was equilibrated with the QM region. During this averaging (100 ns) there were no qualitative changes in the MM structure. In the RS structure we obtained (Figure 1, left, UUU in site, one U in MM region not illustrated) the following H-bond distances between the conserved residues and the phosphate diester structure are short (suggesting strong H-bonds):[84,85] the (ND1)His119−O5′ bond distance, 2.67 Å; the (NE2)His12−O2′ H-bond length, 2.64 Å. The H-bond distance between O1P (NE2) and His12 is 3.22 Å and between Lys41 and His119 and O1P is 4.48 and 3.92 Å, respectively (weak interaction). There is a normal H-bond distance between (NZ)Lys41 and O2′ (2.90 Å). The P−O2′ bond length is 3.07 Å. Note the near in line attack arrangement of O2′, the phosphate and the O5′ species (O2′−P−O5′ angle 160.5°) in the RS supporting speed-up (α-catalysis)[2] and the effective positioning of the conserved residues for possible proton donation and acceptance, Figure 1 (left).

Generating Reaction Paths. Given the RS, Figure 1 (left), reaction paths (mechanisms) to a final PS must be identified. In this system it is expected that the first event in the reaction will be the attack of the O2′ on the adjacent 3′,5′-phosphate diester bond. To find the reaction paths we initiated the reaction (see SI, Sections 2b and 2c) via the variation of two degrees of freedom. Using the relatively unbiased search method discussed in the SI this resulted two quite different minimum energy paths: one (Path 1) corresponding well to the classical reaction mechanism (Scheme 1) and a second reaction path (Path 2) incorporating a triester mechanism (Scheme 2).

dx.doi.org/10.1021/ja406122c | J. Am. Chem. Soc. 2014, 136, 927−936

Table 1. Relevant Bond Orders[62] for Paths 1 and 2

	P−O2′	P−O5′	P−O1P	P−O2P	H(O2′)−O1P	H(O2′)−NE2(His12)	HD1(His119)−O5′
RS	–	1	1	1	–	–	–
Path 1, TS	0.03	0.12	1.01	1.023	0.001	0.43	0.32
Path 2, TS1	0.18	1.0	0.93	0.989	0.15	0.15	–
Path 2, INT	0.84	1.0	0.89	0.977	1.0	–	–
Path 2, TS2	0.86	0.22	0.93	1	0.41	0.26	0.23
PS	1	–	1	1	–	1	1

Path 1 (Scheme 1) was initiated by reducing the length (magnitude) of the P−O2′ dimension (SI Section 4a). This overcame the barrier from the RS while not restricting changes in other atomic degrees of freedom. On further optimization and equilibration the system evolved (without further control) to the PS illustrated in Figure 1 (right). At this point the entire path was reoptimized with iterative thermal averaging (SI, Section 2c) to find the minimum energy reaction path using an NEB[79] method in which the structures along the reaction path (nodes Figure 2) were included in thermal equilibration (SI, Section 2d).

Path 2 (Scheme 2) was initiated by extension of the O2′−H bond starting from the same RS as Path 1. Overcoming the barrier to bond breaking using unrestricted optimization lead to a weakly stable protonated INT (Figure 4, right, note the protonation of O1P by H(O2′)). Further extension of the P−O5′ bond results in the passage to the same PS as Path 1 (Figure 1, right and as discussed below).

The Classical (Minimal) Reaction Path 1. A schematic of reaction Path 1 is given in Scheme 1. This mechanism (classical mechanism) has received wide acceptance in the enzyme catalysis community.[1,6,9,22,86] However, it does not incorporate one of the most important catalytic mechanisms, protonation of a bridging oxygen (in this case O1P), identified in the extensive studies of uncatalyzed analog reactions (β-catalysis)[2,6,25,43] and simulations of similar reactions in solution.[23,50] The Pauling bond orders (BO)[62] in the TS for this mechanism are given in Table 1. The detailed structures along the reaction path are given in SI, Section 4b, and bond length changes in Table 2 and Figure S4.

Table 2. PO Bond Lengths (Å) for TS1 of Path 1 and INT of Path 2

	P−O2′	P−O3′	P−O1P	P−O2P	P−O5′	O2′−O5′
Path 1, TS	2.10	1.58	1.50	1.49	2.33	4.57
Path 2, INT	1.82	1.68	1.61	1.53	1.76	3.57

Perhaps the most important feature of the optimal path calculations for Path 1 is its nearly dissociative A_ND_N character with a very loose TS. This mechanism is very different from the more highly associative $A_N + D_N$ or A_ND_N type mechanisms[58] that have been proposed to explain the uncatalyzed reaction data.[10,16,87] the P−O2′ and P−O5′ reaction coordinate distances in the TS, Table 2 and Figure S4, are shorter (2.10 and 2.33 Å) than a fully dissociative mechanism[62] but similar to those found for kinase reactions which are accepted as dissociative.[60] In the calculations the O2′−O5′ total reaction coordinate is fully flexible and fully optimized (SI, Section 2b). However, the change in this distance is not large as the system passes through the TS structure, Figure 2 and Table 2 (SI, Section 4, Figure S4). The TS coordination and structure of Path 1 are similar to the metaphosphate structures typical of dissociative $D_N + A_N$ reactions.[60,62] The O2′−P−O5′ bond angle in the TS is nearly linear (Figure 2 left and Figure 4S) facilitating attack, α-catalysis.[2,25,28]

The free energies along the NEB optimized[74,79] reaction path and the structure of the TS for Path 1 are given in Figure 2. We note that in the TS there is still a small amount of BO for the P−O2′ and P−O5′ bonds (Table 1, total BO 0.15, Pauling BO).[62]

The interpretation of secondary isotope data by Sowa et al.[86] in terms of BO of the TS is taken as supporting the classical mechanism (Path 1) for the RNase reaction. They interpret their result as weakly associative. We note, however, that the BO of the bridging oxygens that we calculate from the mechanism of Path 1 (Table 1, BO) has a more dissociated TS than the concerted A_ND_N mechanism supported in the Sowa paper.[86] Herschlag[30] has interpreted thio-effects data for the catalyzed reaction as also supporting the classical mechanism. Both these results will be discussed further below. In addition to its highly dissociative character a major problem with this mechanism is its high reaction barrier (25 kcal/mol). This free energy barrier is higher than estimated from data[1,88] for the complete reaction and higher than previously found (using similar calculations)[26] for the hydrolysis reaction (observed to be faster).[1,26] It is also higher than the barriers in the similar $D_N + A_N$ mechanism in kinase reactions.[30,60,89] While the classical reaction path has received wide acceptance,[6,30,47] only three of the four rate enhancing mechanisms (α, γ, and δ-catalysis)[2] identified in studies of solution reactions are implemented.[25] To achieve the observed acceleration would require a near

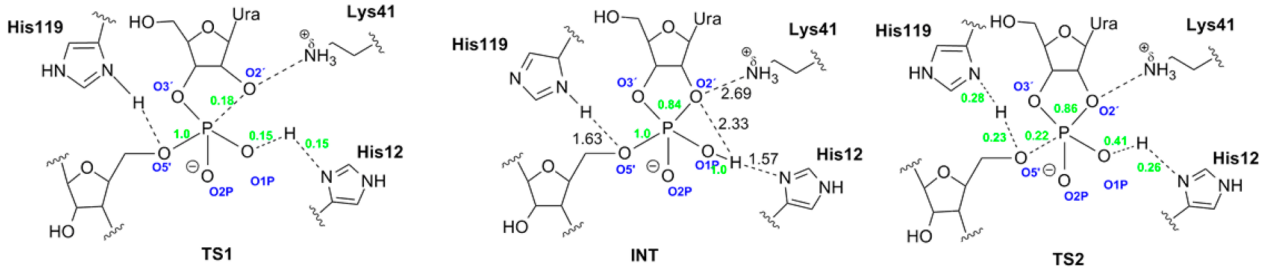

Figure 3. The structures of the transition states (TS1, TS2) and weakly stable intermediate (INT) along Path 2.

dx.doi.org/10.1021/ja406122c | J. Am. Chem. Soc. 2014, 136, 927−936

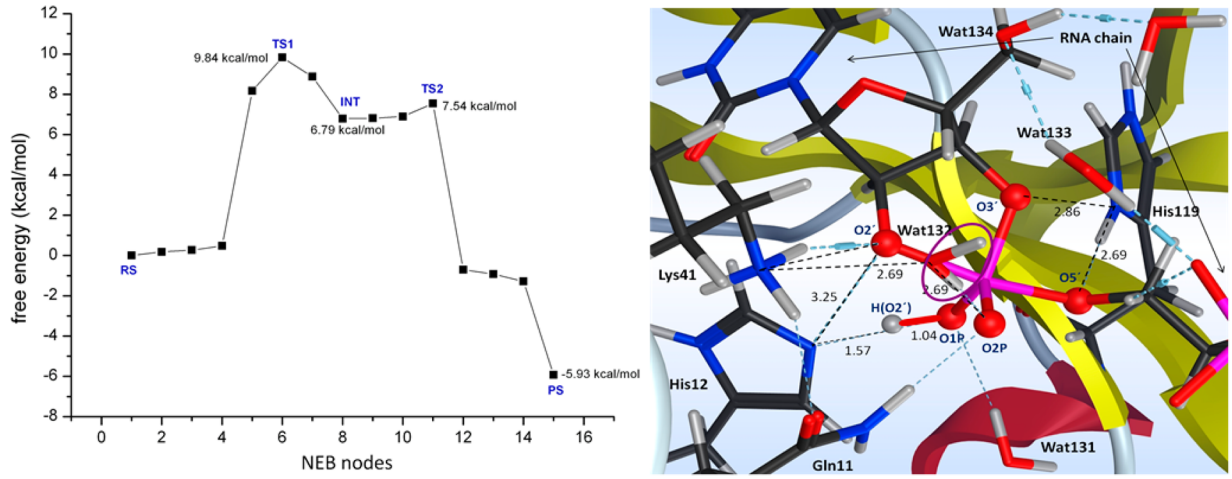

Figure 4. (left) Free energy profile of Path 2. Nodes are points along the reaction coordinate. (right) Weakly stabile intermediate. The active site residues, waters, and two nucleotides of the RNA trimer are represented by sticks, and the TBP phosphorane is depicted as balls and sticks. A zoom-up of the rest of the enzyme is shown as ribbon. The relevant distances are depicted in black. Circled water Lys41 O2P bridge.

Table 3. Relevant O−P−O Bond Angles for TS1 of Path 1 and INT of Path 2

	O2′−P−O3′	O3′−P−O5′	O5′−P−O1P	O1P−P−O2′	O1P−P−O2P	O3′−P−O1P	O3′−P−O2P
Path 1, TS	87.6°	79.3°	85.0°	95.5°	123.5°	116.8°	117.9°
Path 2, INT	86.3°	83.4°	86.5°	91.1°	120.9°	116.4°	122.7°

optimal implementation of these mechanisms (e.g., a more associative TS).[2]

Triester-Like Mechanism, Path 2. Mechanisms for the RNase A RNA cleavage reaction which include proton neutralization of the TS structure (β-catalysis,[2] proton transfer, PT) have been suggested by several investigators[5,9,47,63] and have been supported by experimental observations, gas-phase quantum chemistry calculations,[9,5,47,63] and simulation of similar phosphate reactions in solution.[23] Such a mechanism has also been proposed as the reaction path for the similar RNaseT1 enzyme.[33,90]

In the mechanism of Path 2 (found by NEB optimization and illustrated in Scheme 2, see Section 2 SI) on the initiation of the reaction by extension of the O2′−H bond the O2′ proton (H(O2′)) migrates from the O2′ oxygen to protonate the O1P. Optimization of this pathway lead to a weakly stable phosphorane intermediate (resulting in a triester or "substrate as base"[23,50] mechanism). Schematics of the bond and structure of the TS, TS1, TS2 are given in Figure 3, the intermediate in Figures 3 and 4, and estimates of the free energies (see SI, Section 4c) in Figure 4. (For all NEB structures see SI, Section 4d and bond length changes Figure 5S.)

The most important event in this mechanism is the protonation of the O1P reducing the charge of the structures in the transition region and leading to the associated triester-like weakly stable (<1 kcal/mol) intermediate (INT) structure (Figure 4, right) with quite low barriers (Figure 4, left) and the early (similar to RS) endocyclic TS1 and late (similar to PS) exocyclic TS2 transition states, Figure 4.[2,63] The activation barriers to reach TS1 (10 kcal/mol rate determining) and from the very weakly stable intermediate to reach TS2 (1 kcal/mol, out of intermediate, see Figure 4) are much lower than that of Path 1 due to the reduction of charge by the protonation of O1P. The movement of the NE2 site of the His 12 residue (O1P−NE2 bond length 3.22 Å RS, 2.59 Å INT, and 2.54 Å PS) is an essential part of this shuttle mechanism. Starting from this intermediate structure, extension of the P−O5′ bond completes the reaction with the transfer of the H(O2′) proton to NE2(His12) and the HD(His119) proton to the O5′fragment and, remarkably, leading to the same the PS as Path 1. (RMDS 0.087 see Table 2 and Figure S6, SI). A similar triester mechanism has previously been proposed by Breslow[9] and supported by interpretations of buffer catalyzed reactions.

However, in Breslow's mechanism the TS neutralizing proton comes from His119 rather than from the H(O2′), and this occurs in two steps rather than concerted as in Scheme 2 (see also Figure S5). In the RS of Figure 1 (left) the His119 is too distant from O2P to allow this transfer. We have done extensive simulation without success to try to identify changes in structure that might support the Breslow mechanism.

The changes in the important bond lengths along reaction Path 2 are given in Figure S5, the Pauling BO[62] of the important bonds in the structures along the path in Table 1, and the bond lengths in Table 2. The changes of important coordinates along the reaction path support the separation of the reaction into two processes, first the concerted formation of the INT, Figure 4 right, via TS1. Note the correlation of the H(O2′) proton transfer with the movement of the increasingly nucleophilic O2′ oxygen (e.g., the increase of the O2′−H(O2′ bond distance) with the decrease in the O2′−P distance, Figure S5). In the early TS1, Figure 3, the P−O5′ bond to the leaving group remains fully formed (BO 1.0), O2′ is in an attack position, but the O2′−O1P bond is not yet formed (BO 0.18, Table 1). H(O2′) is in position to coordinate O1P (BO H(O2′)−O1P is 0.15) but is still shared with His12. Throughout the initial passage to the intermediate the distance of the H(O2′) proton from the general base His12 is nearly constant, see the bond lengths changes in Figure S5.

The positions of the conserved residues also change in important ways along the reaction paths. For example, in Path 2 the NE2 site of His12 moves toward O1P in the passage to INT, and it is closer to the O1P (2.59 Å) than in the TS of Path

dx.doi.org/10.1021/ja406122c | J. Am. Chem. Soc. 2014, 136, 927−936

1 (2.78 Å). This supports full transfer of the H(O2′) proton in the INT. The reaction coordinate O2′−O5′ in Path 2 shortens (as opposed to Path 1, see Figures S4 and S5) to facilitate the formation of the associative phosphorane intermediate. This is consistent with observations on uncatalyzed reactions.[2,23,25] In the INT the O1P−H(O2′) bond is fully formed (BO 1.0, Table 1). This is a trigonal pyramid phosphorane structure with normal P−O bonds, the bond angles along the reaction coordinate remain close to linear (Table 3 and Figure S5). The equatorial to axial bond angles are very close to 90° (Table 3). All these are consistent with a phosphorane structure. The apical bonds with lengths 1.81 and 1.76 Å are longer than the equatorial bonds (Table 2) also consistent with the conjectures of Westheimer.[20]

After the weakly bound INT the system moves to TS2. Because the barrier to escape the INT is so low (1 kcal/mol) the presence of this structure probably does not affect the reaction rate, and the effective barrier to reaction is the TS1 height (10 kcal/mol). In TS2 the P−O5′ bond to the leaving group is almost broken (BO 0.22), and the O2′−P bond is almost formed (BO 0.86). However, the O5′ oxyanion is still not protonated HD1(His119)−O5′ (BO 0.23).

After TS2 as the system moves to the PS the H(O2′) proton is finally transferred to the His12 and the His119 proton fully transferred to the leaving RNA fragment. While the motions along the reaction path are concerted, Figure S5 illustrates that the proton transfer from His 119 to the leaving group does not occur until the system has passed through the intermediate. The late protonation of the leaving group is consistent with observations on homogeneous reactions.[2,39,43,50,91]

The NE2(His12)−O1P H-bond is short (2.55 Å) in the PS due to the movement of this ligand deeper into the catalytic pocket. Remarkably, considering the difference in structures along the reaction coordinate and the unbiased optimization of the structures (see SI, Section 2), this lowest energy path[74,79] produces the same PS as in Path 1 (RMSD: 0.087, see SI, Section 5a). All of these movements and structures agree with the classic Westheimer analysis of cleavage-transesterification reactions[20] and with more recent interpretations.[1,3,4,6,8,12,16,23,27,28,36,39,43,45,47,65,87] In addition the final protonation of the PS is correct for the second step in the total RNase A mechanism (the hydrolysis step,[26] Scheme S1, SI).

The free energies[59,60] along reaction Path 2 are illustrated in Figure 4, left. The early rate-determining transition state, TS1, has highest barrier, 10 kcals/mol (peak of point 6). The barrier height out of the INT to the PS, TS2, is quite small (1 kcal), NEB point 11, see SI, Section 4d). The TS1 barrier is considerably lower than that of the Path 1 barrier of 25 kcal/mol, Figure 2, and is less than the rate-determining energy barrier for the hydrolysis step TS2 (13 kcal/mol) in the hydrolysis reaction (step 2 of the RNase A mechanism, calculated with same approach).[26] This is consistent with the observation that the rate of reaction of step 1 is faster than that of step 2.[1,17]

The weakly stable INT supports the observation that no O3′ isomerization is found in the RNase A reaction.[20,25] However, it is possible that sterical effects also play a role in preventing the isomer formation.[25] We note that in our previous calculation on the hydrolysis step[26] we also obtained a weakly bound phosphorane intermediate. However, in this case active site waters in the catalytic cell stabilized the intermediate. That is, for the hydrolysis step no proton transfer was required to neutralize the TS even though a weakly bound intermediate was found. The structures of the TSs here are similar to those recently identified for the reaction path of the uncatalyzed reaction mechanism by Harris.[43]

Two results from direct observations of the catalytic reactions for the RNase A/substrate complex remain to be reconciled with our results. Herschlag[30] reports the effects on the chemical rate, k_{cat}, of thio substitution on the nonbridging phosphate oxygens in the cleavage of UpA by the RNase A enzyme. The isomers of the thio-substituted phosphate diester in this substrate are illustrated in Figure S6 (SI). The lack of a thio effect on the R_6 isomer[92] (thio substitution at the OP2 position) was taken by Herschlag[30] as evidence that the classical mechanism is followed in the RNase reaction. However, in defense of his competing triester mechanism Breslow[8] pointed out that there is a modest 70-fold thio effect reduction in k_{cat} for the S_p isomer (thio substitution at the O1P position also illustrated in Figure S6).[93] In the S_p isomer S replaces the O1P, while in R_p S replaces the O2P. In our mechanism the H(O2′) protonates the O1P so it is expected that replacement of this O by an S would have the largest effect. Breslow[8] suggests that this supports a triester mechanism. A more recent observation of thio substitution effects has been reported for the RNaseT1 enzyme.[33] This is an RNase enzyme (also cleaving RNA at the O3′ position) with a catalytic cell structure similar to RNase A (Glu58 general base, His92 general base). For this enzyme there is a very large thio effect (much larger than for the RNase A reaction), which is accepted as evidence for a triester mechanism. Thio substitution effects relating to the RNase A reaction have also been discussed by Perrin et al.[67]

Results summarizing the calculation of thio substitution effects in small molecular models of transesterification reactions in solutions have been reported. These calculations study small molecule models in solution with a formal dianionic TS (as opposed to mono anionic TS reactions here).[3,44,58,91,94,95] They show modest changes in TS1 (their TS) barrier height on thio substitution of bridging O for these analog reactions. However, it is not clear how to extrapolate these calculations to the enzyme environment leaving the observed thio effects for the RNase reaction difficult to interpret.[23,95,96] At this point we accept our calculations as supporting the conclusions of Breslow.[9] Further simulations using the full enzyme substrate system might clarify these interpretations.

Sowa et al.[86] report O^{18} isotope effect studies on the RNase A phosphate cleavage mechanism. Normal secondary isotope effects are expected to reflect a loss of the BO in the TS.[86] In Sowa's paper the observation of a normal isotope was interpreted as supporting the classical mechanism.[28,86] However, in the optimized reaction path for the classical mechanism, Path 1, we find a highly dissociative mechanism with a near metaphosphate-like TS. Such a TS might be expected to have an increase rather than a loss in BO. Consistent with this we note from Table 1 that our calculations lead to a small increase in the sum of BO for the nonbridging Os in the TS in Path 1 suggesting that this mechanism would lead to an inverse secondary isotope effect. Furthermore, in the triester mechanism, Path 2 (Tables 1 and 2) there is a small decrease in BO (for TS1, TS2 and INT) that could be interpreted as consistent with the normal secondary isotope observed. Theoretical efforts to calculate isotope effects for solution phase analog systems have been reported.[23] These results are also difficult to extrapolate to full enzyme reactions.[25,44,94,97,98] In a recent review of phosphoryl transfer

dx.doi.org/10.1021/ja406122c | J. Am. Chem. Soc. 2014, 136, 927−936

mechanism Kamerlin et al.[23] also conclude that its difficult to interpret TS state dynamics from isotope and thio measurements.

The role of the conserved Lys41 is another controversial part of the mechanism of the RNase enzyme.[1,15,22,99] In their site mutagenesis studies Messmore et al.[15] found that replacement of Lys41 by Cys41 decreases the k_{cat}/K_M to 8% of the wild-type enzyme in the complete mechanism. This supports the conjecture that Lys 41 has a major role in the RNase A mechanism. However, in the simulations of the cleavage-transesterification reaction reported here (first step of the RNase A reaction) the direct interactions of Lys41 with the substrate along the reaction path are not particularly strong. There may be a role for Lys41 in stabilizing the intermediate in this step by building up a strong bridge utilizing water 132 between (NZ)Lys41 and O2P. In the RS the (NZ)Lys41−OW(Wat132) and the OW(Wat132)−O2P H-bond lengths are 2.79 and 2.77 Å, respectively, circled Figure 4, right. Both these H-bonds shorten to 2.69 Å (strong H-bonds) in the intermediate state (see Figure 4, left). Similar water bridges are believed to play an important role in the kinase and other mechanisms.[59,100] The weak thio effects observed in thio substituted reactions have also been taken as evidence of the absence of strong direct H bond interactions with nonbridging oxygens in agreement with the results of these calculations.[30,67]

In our prior calculation of the hydrolysis step in the overall RNase A reaction the Lys41 was found to be the preferred general acid[26] contrary to the normal interpretation of this mechanism. Since the rate-limiting step is the second (hydrolysis) step, this seems to be consistent with the major role of Lys41 in the overall reaction.[25]

In view of the results of this calculation that the RS of the hydrolysis step is very close in structure to the PS of the transesterification step. It is interesting to ask why Lys 41 seems to have a somewhat minor role in the transesterification step and a very important role in the hydrolysis step. As mentioned above, the PS, Figure 1 (right), is in very close agreement (see Figure S8) with the starting configuration used for the hydrolysis step[26] in our prior calculation of the second step in the RNase A mechanism. However, in the PS of the transesterification step the Lys 41 is slightly displaced with respect to its RS positioning in the hydrolysis step leading to weaker interaction. When the O5′ hydroxyl RNA fragment is removed from the catalytic cell[26] and the system reoptimized, the Lys 41 repositions in the PS from a NZ(Lys41)−O2′ H-bond of length 3.10 Å in the PS of Paths 1 and 2 to 2.80 Å and in the RS state of the hydrolysis reaction (see Figure S9). This bond length further shortens to 2.60 Å in the PS of the hydrolysis step to facilitate its role as a general acid. This change in structure is discussed in the SI, Section 5c, and illustrated in Figures S8 and S9.

The reoptimized structure (from the PS of this reaction) is essentially identical to that of the RS of the hydrolysis step used in our prior calculation as illustrated in Figure S8 (RMSD, 0.418). This also supports the possibility that the final product in the overall RNase A cleavage reaction may result from the continuation of the reaction without desorption.

CONCLUSION

The RNase A enzyme selectively catalyzes the cleavage of the 3′-5′ backbone phosphodiester bond of RNA with a 10^{12} acceleration. This impressive efficiency and the more recent discoveries of similar reactions in ribozymes[2,101] have led to extensive study of this reaction and various analog reactions.[4,18,23,27,33,58,91] Despite this intensive research for over 60 years the mechanism responsible for this impressive increase in rate is not fully understood. Two competing reaction paths have been vigorously discussed. The classical mechanism that receives the broadest acceptance[1,5,16,27,30] in the enzyme community follows a minimal acid/base mechanism with a dianionic TS (Scheme 1, Scheme S2). The second reaction path that has been proposed[5,8] is based on a triester mechanism leading to a monoanionic TS. This mechanism has received less acceptance. However, there is universal support for triester cleavage-transesterification mechanisms in the low to medium pH region in catalyzed and uncatalyzed reactions in homogeneous solutions.[5,8,16,45,47,48,50]

In this article computational results (QM/MM[46,50,61]) are reported that identify, via a fairly unbiased search, two lowest energy reaction paths for the RNase A reaction in the enzyme substrate complex, each of which resembles one of these mechanisms. In these calculations full movement with thermal averaging is allowed for all the atomic species in both the QM and MM regions. In the method implemented the variations of all bond lengths along the reaction paths are obtained. Thus the proton motions that are the key to differentiating these mechanisms are fully described along a thermally averaged minimum energy reaction path forming optimal structures in either mechanism. The detailed motion of conserved residues degrees of freedom (particularly His12) in the catalytic region is important to the proton transfer and the low barriers in the transition region of Path 2. The energetics calculated from these simulations using a very reliable level of computational accuracy (B3LYP), a large representation of the catalytic regions (QM region), and full representation of the remaining protein and solvent strongly support the presently less accepted triester mechanism, Path 2, Scheme 2 above.

The optimized reaction path for this mechanism leads to a weakly stable intermediate with low TS barrier (10 kcal/mol) and an associative $A_N + D_N$ concerted mechanism.[58] The alternative mechanism, similar to the classical path, Path 1, Scheme 1, while providing a legitimate minimum free energy path based on the same general acid and base as for Path 2 and arriving at the same PS, results in a reaction barrier that is very high (25 kcals/mol) and a TS with a near dissociative structure, both of which are inconsistent with observations.[3,6,8,9,16,45] Paths 1 and 2 are calculated with the same theory without additional approximations and, therefore, can be reliably compared. We note that the differences in barrier heights that we report would lead to an increase in the chemical rate by a factor of roughly 10^{11}, illustrating the importance correctly interpreting the structures encountered along the reaction path.

Additional support for the triester mechanism has been provided by the observations of Piatek, Gray, and Anslyn[34] that the pK_a of a phosphorane species is predicted to be higher than various proton donors in the vicinity of the reaction suggesting the formation of a triester species (donation of a proton to the nonbridging phosphate O) where possible. The assertion of Piatek et al.[34] is supported by computational results[102,103] and by estimations from pK_a data for related systems.[102] Further support for the triester mechanism for the RNase A reaction comes from the thio observations of Loverix et al.[51] which strongly support a triester mechanism for the RNase T1 enzyme which has catalytic region closely resembling that of RNase A.

While the electronic structure methods we have employed are not without error, they are expected to be accurate within a few kcals/mol (far less than the 15 kcal/mol difference in barrier between Paths 1 and 2) and provide atom position estimates accurate within 0.1 of an Å.[104,105] In addition these methods (generally considered to be very reliable in the quantum chemistry community) have been tested against known structural data for systems similar to those studied here and shown to provide very good accuracy in similar catalytic simulations.[26,51] Because of the complexity of the interactions expected to be encountered in this system, we used a very large QM zone and a relatively high level first-principle-based quantum chemistry approximation. All atomic positions in the QM and MM zones are thermally optimized along the minimum energy reaction path thermal iteration of the reaction path to convergence (see SI, Section 2).

An important requirement for this kind of study (and a potential problem for our interpretation) is the determination of a starting structure, RS, from the data available. In this case we were not able to find X-ray data close to the RS for the cleavage transesterification reaction. The structure used to initiate the simulation for this calculation was derived from the X-ray data for related systems, extensive docking simulations and long equilibration of the system. The RS that we use was the only acceptable candidate that we found (see SI, Section 3 for the validation procedure). This choice without further guidance produced a PS (same for both paths) that is essentially identical to the starting state we developed in a recent simulation of the hydrolysis step (second step of the RNase A) reaction.[26] In addition a novel interpretation of the role of Lys41 was identified.

While there are questions as to the correctness of our RS and this could effect the results, we believe that we have done as much as possible with the available structure data and that this interpretation is at least as reliable as the structural information used in the more qualitative interpretations of data for this system.

Given the present state of understanding the structures of the enzyme substrate complex structure and the magnitudes of the calculated differences in TS barrier heights these results strongly support the triester mechanism despite the present general acceptance of the classical mechanism. Since this is an exceedingly well studied reaction mechanism the still existing controversies over essential points in the interpretation are especially important to resolve.

■ ASSOCIATED CONTENT

Supporting Information

Detailed description of the computational methods, the analysis of structural data, the optimization of the RS, TS, INT and NEB structures, etc. This material is available free of charge via the Internet at http://pubs.acs.org.

■ AUTHOR INFORMATION

Corresponding Author

jweare@ucsd.edu

Notes

The authors declare no competing financial interest.

■ ACKNOWLEDGMENTS

The calculations were carried out at the MSCF in the EMSL User Facility sponsored by the U.S. DOE. The authors thank the DFG (German Research Foundation) for the financial support of B.E.

■ REFERENCES

(1) Raines, R. T. *Chem. Rev.* **1998**, *98*, 1045−1065.
(2) Emilsson, G. M.; Nakamura, S.; Roth, A.; Breaker, R. R. *RNA* **2003**, *9*, 907−918.
(3) Hengge, A. C.; Tobin, A. E.; Cleland, W. W. *J. Am. Chem. Soc.* **1995**, *117*, 5919−5926.
(4) Wladkowski, B. D.; Ostazeski, P.; Chenoweth, S.; Broadwater, S. J.; Krauss, M. *J. Comput. Chem.* **2003**, *24*, 1803−1811.
(5) Glennon, T. M.; Warshel, A. *J. Am. Chem. Soc.* **1998**, *120*, 10234−10247.
(6) Anslyn, E.; Breslow, R. *J. Am. Chem. Soc.* **1989**, *111*, 5972−5973.
(7) Breslow, R. *Acc. Chem. Res.* **1991**, *24*, 317−324.
(8) Breslow, R. *Proc. Natl. Acad. Sci. U.S.A.* **1993**, *90*, 1208−1211.
(9) Breslow, R.; Chapman, W. H. *Proc. Natl. Acad. Sci. U.S.A.* **1996**, *93*, 10018−10021.
(10) Breslow, R.; Dong, S. D.; Webb, Y.; Xu, R. *J. Am. Chem. Soc.* **1996**, *118*, 6588−6600.
(11) Chatani, E.; Tanimizu, N.; Ueno, H.; Hayashi, R. *J. Biochem.* **2001**, *129*, 917−922.
(12) Deakyne, C. A.; Allen, L. C. *J. Am. Chem. Soc.* **1979**, *101*, 3951−3959.
(13) Delcardayre, S. B.; Ribo, M.; Yokel, E. M.; Quirk, D. J.; Rutter, W. J.; Raines, R. T. *Protein Eng.* **1995**, *8*, 261−273.
(14) Herries, D. G.; Mathias, A. P.; Rabin, B. R. *Biochem. J.* **1962**, *85*, 127−134.
(15) Messmore, J. M.; Fuchs, D. N.; Raines, R. T. *J. Am. Chem. Soc.* **1995**, *117*, 8057−8060.
(16) Perreault, D.; Anslyn, E. *Angew. Chem., Int. Ed.* **1997**, *36*, 432−450.
(17) Raines, R. T. *Nucleic Acids Mol. Biol.* **2004**, *13*, 19−32.
(18) Thompson, J. E.; Venegas, F. D.; Raines, R. T. *Biochemistry* **1994**, *33*, 7408−7414.
(19) Trautwein, K.; Holliger, P.; Stackhouse, J.; Benner, S. A. *FEBS Lett.* **1991**, *281*, 275−277.
(20) Westheimer, F. *Acc. Chem. Res.* **1968**, *1*, 70.
(21) Dennis, E. A.; Westheim., Fh *J. Am. Chem. Soc.* **1966**, *88*, 3431.
(22) Perrin, C. *J. Org. Chem.* **1995**, *60*, 1239−1243.
(23) Kamerlin, S. C. L.; Sharma, P. K.; Prasad, R. B.; Warshel, A. *Q. Rev. Biophys.* **2013**, *46*, 1−132.
(24) Fedor, M. J. *Annual Review of Biophysics* **2009**, *38*, 271−299.
(25) Lonnberg, H.; Stromberg, R.; Williams, A. *Organic & Biomolecular Chemistry* **2004**, *2*, 2165−2167.
(26) Elsaesser, B.; Valiev, M.; Weare, J. H. *J. Am. Chem. Soc.* **2009**, *131*, 3869−3871.
(27) Fedor, M. J.; Williamson, J. R. *Nat. Rev. Mol. Cel. Biol.* **2005**, *6*, 399−412.
(28) Cleland, W. W.; Hengge, A. C. *Chem. Rev.* **2006**, *106*, 3252−3278.
(29) Zalatan, J. G.; Herschlag, D. *J. Am. Chem. Soc.* **2006**, *128*, 1293−1303.
(30) Herschlag, D. *J. Am. Chem. Soc.* **1994**, *116*, 11631−11635.
(31) Langen, R.; Schweins, T.; Warshel, A. *Biochem.* **1992**, *31*, 8691−8696.
(32) Schweins, T.; Langen, R.; Warshel, A. *Str. Biol.* **1994**, *1*, 476−484.
(33) Loverix, S.; Winqvist, A.; Stromberg, R.; Steyaert, J. *Chemistry & Biology* **2000**, *7*, 651−658.
(34) Piatek, A. M.; Gray, M.; Anslyn, E. V. *J. Am. Chem. Soc.* **2004**, *126*, 9878−9879.
(35) Borah, B.; Chen, C. W.; Egan, W.; Miller, M.; Wlodawer, A.; Cohen, J. S. *Biochemistry* **1985**, *24*, 2058−2067.
(36) Cleland, W. W.; Hengge, A. C. *Faseb Journal* **1995**, *9*, 1585−1594.
(37) Ladner, J. E.; Wladkowski, B. D.; Svensson, L. A.; Sjolin, L.; Gilliland, G. L. *Acta Crystallogr., Sect. D: Biol. Crystallogr.* **1997**, *53*, 290−301.

(38) Lahiri, S. D.; Zhang, G. F.; Dunaway-Mariano, D.; Allen, K. N. *Science* **2003**, *299*, 2067−2071.
(39) Oivanen, M.; Kuusela, S.; Lonnberg, H. *Chem. Rev.* **1998**, *98*, 961−990.
(40) Witzel, H. *Angew. Chem., Int. Ed.* **1963**, *75*, 686.
(41) Wlodawer, A.; Sjolin, L. *Biochemistry* **1983**, *22*, 2720−2728.
(42) Field, M. J.; Bash, P. A.; Karplus, M. *J. Comput. Chem.* **1990**, *11*, 700−733.
(43) Harris, M. E.; Dai, Q.; Gu, H.; Kellerman, D. L.; Piccirilli, J. A.; Anderson, V. E. *J. Am. Chem. Soc.* **2010**, *132*, 11613−11621.
(44) Lopez, X.; York, D. M.; Dejaegere, A.; Karplus, M. *Int. J. Quantum Chem.* **2002**, *86*, 10−26.
(45) Taira, K.; Uchimaru, T.; Tanabe, K.; Uebayasi, M.; Nishikawa, S. *Nucleic Acids Res.* **1991**, *19*, 2747−2753.
(46) Warshel, A.; Levitt, M. *J. Mol. Biol.* **1976**, *103*, 227−249.
(47) Wladkowski, B. D.; Krauss, M.; Stevens, W. J. *J. Am. Chem. Soc.* **1995**, *117*, 10537−10545.
(48) Wladkowski, B. D.; Krauss, M.; Stevens, W. J. *J. Phys. Chem.* **1995**, *99*, 6273−6276.
(49) Klahn, M.; Rosta, E.; Warshel, A. *J. Am. Chem. Soc.* **2006**, *128*, 15310−15323.
(50) Kamerlin, S. C. L.; Haranczyk, M.; Warshel, A. *J. Phys. Chem. B* **2009**, *113*, 1253−1272.
(51) Plotnikov, N. V.; Prasad, B. R.; Chakrabarty, S.; Chu, Z. T.; Warshel, A. *J. Phys. Chem. B* **2013**, *117*, 12807−12819.
(52) Glaves, R.; Mathias, G.; Marx, D. *J. Am. Chem. Soc.* **2012**, *134*, 6995−7000.
(53) Grigorenko, B. L.; Rogov, A. V.; Nemukhin, A. V. *J. Phys. Chem.. B* **2006**, *110*, 4407−4412.
(54) Li, W.; Rudack, T.; Gerwert, K.; Gräter, F.; Schlitter, J. *J. Chem. Theory Comput.* **2012**, *8*, 3596−3604.
(55) Prasad, B. R.; Plotnikov, N. V.; Warshel, A. *J. Phys. Chem. B* **2013**, *117*, 153−163.
(56) Kluger, R.; Covitz, F.; Dennis, E.; Williams, L.; Westheim, F. *J. Am. Chem. Soc.* **1969**, *91*, 6066.
(57) Kluger, R.; Westheim, F. *J. Am. Chem. Soc.* **1969**, *91*, 4143−&.
(58) Hengge, A.; Onyido, I. *Curr. Org. Chem.* **2005**, *9*, 61−74.
(59) Valiev, M.; Kawai, R.; Adams, J. A.; Weare, J. H. *J. Am. Chem. Soc.* **2003**, *125*, 9926−9927.
(60) Valiev, M.; Yang, J.; Adams, J. A.; Taylor, S. S.; Weare, J. H. *J. Phys. Chem. B* **2007**, *111*, 13455−13464.
(61) Ranaghan, K. E.; Mulholland, A. J. *Int. Rev. Phys. Chem.* **2010**, *29*, 65−133.
(62) Mildvan, A. S. *Proteins: Struct., Funct., Genet.* **1997**, *29*, 401−416.
(63) Lim, C.; Tole, P. *J. Am. Chem. Soc.* **1992**, *114*, 7245−7252.
(64) Wladkowski, B. D.; Svensson, L. A.; Sjolin, L.; Ladner, J. E.; Gilliland, G. L. *J. Am. Chem. Soc.* **1998**, *120*, 5488−5498.
(65) Glennon, T. M.; Warshel, A. *Biophys. J.* **1999**, *76*, A180−A180.
(66) Haydock, K.; Lim, C.; Brunger, A. T.; Karplus, M. *J. Am. Chem. Soc.* **1990**, *112*, 3826−3831.
(67) Thomas, J. M.; Yoon, J. K.; Perrin, D. M. *J. Am. Chem. Soc.* **2009**, *131*, 5648−5658.
(68) Trawick, B. N.; Daniher, A. T.; Bashkin, J. K. *Chem. Rev.* **1998**, *98*, 939−960.
(69) Gilbert, W. *Nature* **1986**, *319*, 618−618.
(70) Lilley, D. M. J. *Biochem. Soc. Trans.* **2011**, *39*, 641−646.
(71) Robertson, M. *BMC Biol.* **2010**, 8.
(72) Salehi-Ashtiani, K.; Luptak, A.; Litovchick, A.; Szostak, J. W. *Science* **2006**, *313*, 1788−1792.
(73) Elsaesser, B.; Fels, G. *J. Mol. Model.* **2011**, *17*, 1953−1962.
(74) Henkelman, G.; Jonsson, H. *J. Chem. Phys.* **2000**, *113*, 9978−9985.
(75) Valiev, M.; Bylaska, E.; Tsemekman, K.; Bogatko, S.; Weare, J. *Geochim. Cosmochim. Acta* **2005**, *69*, A511−a511.
(76) Valiev, M.; Garrett, B. C.; Tsai, M. K.; Kowalski, K.; Kathmann, S. M.; Schenter, G. K.; Dupuis, M. *J. Chem. Phys.* **2007**, *127*, 51102.
(77) Zhang, Y. K.; Lee, T. S.; Yang, W. T. *J. Chem. Phys.* **1999**, *110*, 46−54.
(78) Zhang, Y. K.; Liu, H. Y.; Yang, W. T. *J. Chem. Phys.* **2000**, *112*, 3483−3492.
(79) Henkelman, G.; Uberuaga, B. P.; Jonsson, H. *J. Chem. Phys.* **2000**, *113*, 9901−9904.
(80) Klahn, M.; Braun-Sand, S.; Rosta, E.; Warshel, A. *J. Phys. Chem. B* **2005**, *109*, 15645−15650.
(81) Vitagliano, L.; Merlino, A.; Zagari, A.; Mazzarella, L. *Protein Sci.* **2000**, *9*, 1217−1225.
(82) Wlodawer, A.; Miller, M.; Sjolin, L. *Proc. Natl. Acad. Sci. U.S.A.* **1983**, *80*, 3628−3631.
(83) Elsaesser, B.; Fels, G. *J. Mol. Model.* **2010**, *17*, 1953−1962.
(84) Brown, I. D. *Acta Crystallogr.* **1976**, *A*, 24−31.
(85) Schutz, C. N.; Warshel, A. *Proteins: Struct., Funct., Bioinf.* **2004**, *55*, 711−723.
(86) Sowa, G. A.; Hengge, A. C.; Cleland, W. W. *J. Am. Chem. Soc.* **1997**, *119*, 2319−2320.
(87) Gerratana, B.; Sowa, G. A.; Cleland, W. W. *J. Am. Chem. Soc.* **2000**, *122*, 12615−12621.
(88) Eftink, M. R.; Biltonen, R. L. *Biochemistry* **1983**, *22*, 5123−5150.
(89) Smith, G. K.; Ke, Z. H.; Guo, H.; Hengge, A. C. *J. Phys. Chem. B* **2011**, *115*, 13713−13722.
(90) Zegers, I.; Maes, D.; Daothi, M. H.; Poortmans, F.; Palmer, R.; Wyns, L. *Protein Sci.* **1994**, *3*, 2322−2339.
(91) Lonnberg, T.; Lonnberg, H. *Curr. Opin. Chem. Biol.* **2005**, *9*, 665−673.
(92) Burgers, P. M. J.; Eckstein, F. *Biochemistry* **1979**, *18*, 450−454.
(93) Burgers, P. M. J.; Eckstein, F. *Biochemistry* **1979**, *18*, 592−596.
(94) Gregersen, B. A.; Lopez, X.; York, D. M. *J. Am. Chem. Soc.* **2003**, *125*, 7178−7179.
(95) Lonnberg, H. *Org. Biomol. Chem.* **2011**, *9*, 1687−1703.
(96) Hondal, R. J.; Zhao, Z.; Riddle, S. R.; Kravchuk, A. V.; Liao, H.; Bruzik, K. S.; Tsai, M. D. *J. Am. Chem. Soc.* **1997**, *119*, 9933−9934.
(97) Liu, Y.; Gregersen, B. A.; Hengge, A.; York, D. M. *Biochemistry* **2006**, *45*, 10043−10053.
(98) Formoso, E.; Matxain, J. M.; Lopez, X.; York, D. M. *J. Phys. Chem. B* **2010**, *114*, 7371−7382.
(99) Messmore, J. M.; Raines, R. T. *J. Am. Chem. Soc.* **2000**, *122*, 9911−9916.
(100) Utas, J. E.; Kritikos, M.; Sandström, D.; Åkermark, B. *Biochim. Biophys. Acta, Bioenerg.* **2006**, *1757*, 1592−1596.
(101) Lonnberg, T. *Chem.—Eur. J.* **2011**, *17*, 7140−7153.
(102) Davies, J. E.; Doltsinis, N. L.; Kirby, A. J.; Roussev, C. D.; Sprik, M. *J. Am. Chem. Soc.* **2002**, *124*, 6594−6599.
(103) Lopez, X.; Schaefer, M.; Dejaegere, A.; Karplus, M. *J. Am. Chem. Soc.* **2002**, *124*, 5010−5018.
(104) Zhao, Y.; Truhlar, D. G. *Acc. Chem. Res.* **2008**, *41*, 157−167.
(105) Burke, K.; Wagner, L. O. *Int. J. Quantum Chem.* **2013**, *113*, 96−101.